

Interacting dark energy constraints from the full-shape analyses of BOSS DR12 and DES Year 3 measurements

M. Tsedrik^{1,2}, ^{*} S. Lee³, K. Markovic³, P. Carrilho¹, A. Pourtsidou^{1,2}, C. Moretti^{4,5,6}, B. Bose^{1,2}, E. Huff³, A. Robertson⁷, P. L. Taylor^{8,9,10}, J. Zuntz¹

¹*Institute for Astronomy, University of Edinburgh, Royal Observatory, Blackford Hill, Edinburgh, EH9 3HJ, UK*

²*Higgs Centre for Theoretical Physics, School of Physics and Astronomy, Edinburgh, EH9 3FD, UK*

³*Jet Propulsion Laboratory, California Institute of Technology, 4800 Oak Grove Drive, Pasadena, CA 91109, USA*

⁴*SISSA - International School for Advanced Studies, Via Bonomea 265, 34136 Trieste, Italy*

⁵*Centro Nazionale ‘High Performance Computer, Big Data and Quantum Computing’*

⁶*INAF - Osservatorio Astronomico di Trieste, Via Tiepolo 11, I-34143 - Trieste, Italy*

⁷*Observatories, Carnegie Institution for Science, 813 Santa Barbara Street, Pasadena, CA 91101, USA*

⁸*Center for Cosmology and AstroParticle Physics (CCAPP), The Ohio State University, Columbus, OH 43210, USA*

⁹*Department of Physics, The Ohio State University, Columbus, OH 43210, USA*

¹⁰*Department of Astronomy, The Ohio State University, Columbus, OH 43210, USA*

Accepted XXX. Received YYY; in original form ZZZ

ABSTRACT

Dark Scattering (DS) is an interacting dark energy model characterised by pure momentum exchange between dark energy and dark matter. It is phenomenologically interesting because it is unconstrained by CMB data and can alleviate the S_8 tension. We derive constraints on cosmological and DS parameters using three two-point correlation functions (3×2pt) from the Dark Energy Survey third year data release (DES Y3). We then add information from the multipoles of the galaxy power spectrum combined with Baryonic Acoustic Oscillation (BAO) measurements using the twelfth data release of the Baryon Oscillation Spectroscopic Survey (BOSS DR12) and external BAO measurements. We compare results from the direct combination of the probes with the joint posterior distribution calculated with a normalising flow approach. Additionally, we run a CMB analysis with the Planck Public Release 4 (PR4) for comparison of the cosmological constraints. Overall, we find that the combination of probes allows minimising the projection effects and improves constraints without the need to include CMB information. It brings the marginalised posterior maxima closer to the corresponding best-fit values and weakens the sensitivity to the priors of the spectroscopic modelling nuisance parameters. These findings are highly relevant in light of forthcoming data of surveys like DESI, Euclid, and Rubin.

Key words: cosmology:theory – cosmology: observations – large-scale structure of the Universe – methods:statistical

1 INTRODUCTION

Data from the latest generation of cosmological surveys, such as [DESI](#), [Euclid](#) and [Rubin](#) will shed light on the nature of the dark sector (dark energy and dark matter) by providing Large Scale Structure (LSS) information with unprecedented precision. These surveys will allow us to draw unambiguous conclusions about the current cosmological tensions, for example the so-called S_8 tension: a $\sim 2\sigma$ disagreement in the amplitude of matter fluctuations between the one measured in LSS experiments ([Heymans et al. 2021](#); [Abbott et al. 2022a](#)) and the one measured with the CMB and propagated to later times using the standard cosmological model ([Planck Collaboration et al. 2020](#)).

Dark Scattering (DS, [Simpson 2010](#); [Pourtsidou et al. 2013](#)) is one of the potential ‘new physics’ solutions for the S_8 tension. It is a subclass of models, in which dark energy is coupled to cold dark matter via a momentum-exchange interaction. Theoretical modelling

for observables in the DS model has been extensively tested on simulations and applied to data ([Pourtsidou & Tram 2016](#); [Bose et al. 2018](#); [Bose & Taruya 2018](#); [Carrilho et al. 2021](#); [Carrilho et al. 2022](#); [Spurio Mancini & Pourtsidou 2022](#); [Linton et al. 2022](#); [Tsedrik et al. 2023](#); [Carrilho et al. 2023](#); [Carrion et al. 2024](#)). In this work, we provide constraints on DS cosmology with DES Y3, a photometric dataset consisting of three two-point correlation functions: cosmic shear, galaxy clustering, and the cross-correlation of source galaxy shear with lens galaxy positions. We then showcase the power of combining it with a full-shape analysis using data from BOSS DR12, a spectroscopic dataset consisting of three power spectrum multipoles and BAOs. For reference, we also provide constraints on the standard cosmological model, Λ CDM.

2 MODEL

Dark Scattering is an interacting dark energy model, in which dark energy and cold dark matter exchange momentum via elastic scatter-

* mtsedrik@ed.ac.uk

ing (Simpson 2010; Pourtsidou et al. 2013; Skordis et al. 2015). No energy transfer between those two species is involved in the scattering process, hence leaving the expansion history unaffected by the interaction. Additionally, this form of coupling only weakly affects the CMB and is in remarkable agreement with Planck measurements (Pourtsidou & Tram 2016). The DS model is characterised by two extra parameters with respect to Λ CDM: the equation of state parameter, w , and the interaction parameter, ξ . The interaction parameter is defined as the ratio between the scattering cross section and the dark matter mass. For simplicity we take the dark energy equation of state parameter to be constant. For the case of constant w , the Friedmann equation in a flat universe is given by

$$H^2 = H_0^2 \left(\Omega_m a^{-3} + \Omega_{\text{DE}} a^{-3(1+w)} \right), \quad (1)$$

where $H = \dot{a}/a$ is the Hubble rate with the scale factor $a = 1/(1+z)$, the dot denotes a derivative with respect to cosmic time, and H_0 is the value of the expansion rate today; Ω_m is the matter density parameter today and $\Omega_{\text{DE}} = 1 - \Omega_m$ is the dark energy density parameter. The total matter fraction includes contributions from cold dark matter (Ω_c), baryons (Ω_b) and massive neutrinos (Ω_ν).

The interaction between dark matter particles and the dark energy fluid manifests itself through an additional friction or drag in the movement of dark matter particles. Under the assumption of the dark energy speed of sound being equal to the speed of light, we can write the linearised Euler equation as

$$a \partial_a \Theta + \left(2 + (1+w) \xi \frac{\rho_{\text{DE}}}{H} + \frac{a \partial_a H}{H} \right) \Theta + \frac{\nabla^2 \Phi}{a^2 H^2} = 0. \quad (2)$$

Here ∂_a is the derivative with respect to the scale factor, $\Theta = \theta_c/aH$ with θ_c the dark matter velocity divergence, Φ is the corresponding gravitational potential, and ρ_{DE} is the dark energy density. We evolve baryons and dark matter as a single species.

From Equation 1 and Equation 2 we find the linear growth factor, D , and the growth rate $f = d \ln D / d \ln a$ by solving the linearised growth equation. In Equation 2, we see that if $w \approx -1$ the drag/friction-term becomes negligible and the scattering parameter ξ becomes unconstrained. For this reason, in our analysis we vary the combined parameter $A_{\text{ds}} = (1+w)\xi$, with a well-defined Λ CDM-limit of $A_{\text{ds}} = 0$ b GeV^{-1} and $w = -1$. Since ξ is always positive (or zero), the sign of A_{ds} and $(1+w)$ has to be the same. The parameter space region that can resolve the S_8 tension corresponds to $A_{\text{ds}} > 0$ and $w > -1$. In this case, the linear growth factor decreases with respect to the Λ CDM scenario at low redshifts. This leads to a scale-independent suppression of the power spectrum at large scales in DS. However, on smaller scales, in collapsed objects, dark matter particles experience additional friction, which leads to a scale-dependent enhancement of structure growth. Such nonlinear behaviour is modelled within the halo model reaction framework (Cataneo et al. 2019; Bose et al. 2020), which was tested against the DS N-body simulations presented in Baldi & Simpson (2015, 2017) (see also Palma & Candlish 2023).

3 DATA AND METHODS

We consider the publicly released measurements of the three two-point correlation functions (3×2 pt) from DES Y3 (Abbott et al. 2022b, 2023b). They contain cosmic shear, galaxy clustering and galaxy-galaxy lensing information from sources in 4 redshift-bins and lenses from the first 4 redshift-bins of the MagLim sample (Porredon et al. 2021). The corresponding covariance matrix is obtained analytically as described and validated in Friedrich et al. (2021). We

use the same scale-cuts as in the DES Y3 Λ CDM baseline analysis, since we apply the reaction approach, a robust prescription of nonlinearities for DS (Carrilho et al. 2022). The study of these scale-cuts is presented in Krause et al. (2021) and justifies the fact that we do not model effects of baryonic feedback on small scales. We use the official DES-pipeline, CosmoSIS, in which we substitute the computation of linear and nonlinear matter power spectra by CAMB (Lewis & Challinor 2011) with an emulator, DS-emulator. This emulator is discussed in detail in Carrion et al. (2024), where it is also applied to the shear data of the Kilo-Degree Survey (KiDS-1000, Joachimi et al. 2021; Akgari et al. 2021). For DS (and Λ CDM being a DS limit with $w = -1$ and $A_{\text{ds}} = 0$), the DS-emulator provides linear power spectra trained on CLASS (Lesgourgues 2011; Blas et al. 2011) outputs, and nonlinear power spectra trained on ReACT outputs. Both models are trained with CosmoPower (Spurio Mancini et al. 2022). The emulation error is under 1% at all scales of interest.

In the following bullet-points we summarise the difference with respect to the analysis set-up from Abbott et al. (2022b).

- Modelling of the nonlinear power spectrum is done with HMCode2020 (Mead et al. 2021) for Λ CDM motivated by a better agreement with numerical simulations (Abbott et al. 2023a).
- The priors are identical to the ones summarised in Table 1 of Abbott et al. (2022b), except of $\{\Omega_b, h, w\}$ (for instance, $w \in [-1.3, -0.7]$). For these parameters we have narrower flat priors, explained by the parameter-range in the training set of the DS-emulator. Additionally, the prior on the interaction parameter is $A_{\text{ds}} \in [-30, 30]$ b GeV^{-1} , motivated by the constraints found in Carrilho et al. (2023); Carrion et al. (2024).
- We fix the total mass of one massive and two massless neutrinos to $M_\nu = 0.06$ eV. This analysis choice is motivated by the weak constraints from Stage III surveys (Abbott et al. 2022b; Moretti et al. 2023). Moreover, varying M_ν introduces additional prior volume effects (Porredon et al. 2022).
- We do not include information from the small-scale shear ratio (Sánchez et al. 2022) motivated by Aricò et al. (2023).

Additionally, we consider the galaxy power spectrum multipoles from BOSS DR12 (Alam et al. 2015; Gil-Marín et al. 2016; Beutler et al. 2017). The data consists of two galaxy samples: CMASS and LOWZ with effective redshifts $z_1 = 0.38$ and $z_3 = 0.61$, respectively. Each sample covers two different sky cuts, NGC and SGC. Hence in total, we fit 4 independent sets of multipoles. The multipole measurements and covariance are provided in Philcox & Ivanov (2022) and are obtained with the windowless estimator (Philcox 2021a,b). The covariance is based on 2048 ‘MultiDark-Patchy’ mock catalogues (Kitaura et al. 2016; Rodríguez-Torres et al. 2016). Complementarily, we use BAO data from BOSS DR12 (with a cross-covariance, both provided by Philcox & Ivanov 2022), as well as pre-reconstruction BAO measurements at low redshift from the 6DF survey (Beutler et al. 2011) at $z \approx 0.11$ and SDSS DR7 MGS (Ross et al. 2015) at $z = 0.15$. We also add information from high redshift measurements of the Hubble factor and angular diameter distance from the Ly- α forest auto and cross-correlation with quasars from eBOSS DR16 (du Mas des Bourboux et al. 2020) at $z \approx 2.33$. Further in text ‘FS+BAO’ means the full shape (FS) analysis with the BOSS DR12 data with the inclusion of all BAOs mentioned above.

For the BOSS DR12 FS analysis we add an EFTofLSS (Baumann et al. 2012; Carrasco et al. 2012; Perko et al. 2016; Fonseca de la Bella et al. 2017; D’Amico et al. 2020) modelling module to CosmoSIS. The modelling code is discussed in detail in Moretti et al. (2023). It was also extensively validated on N-body simulations in Λ CDM (Oddo et al. 2020, 2021; Rizzo et al. 2023; Tsedrik

Table 1. Mean values and 68% c.l. values for DS and Λ CDM with fixed one massive neutrino with $M_\nu = 0.06$ eV for the different probes and their combination considered in this work. We show the MAP values in parentheses, and include derived constraints on σ_8 . We report the number of data-points N_{data} , the number of parameters N_{par} varied in the MCMC and number of analytically marginalised parameters in parentheses, χ^2 and χ^2_{prior} computed with MAP-values and log-evidence log \mathcal{Z} from the sampler. Unconstrained parameters are denoted by a dash-line. The BBN prior is applied in the FS+BAO and joint analyses.

N_{data}	3 \times 2pt from DES Y3		FS + BAO from BOSS DR12 and external BAOs		joint	
	Λ CDM	DS	Λ CDM	DS	Λ CDM	DS
	462		456+(8+4)		930	
Ω_m	0.305 ± 0.024 (0.317)	0.303 ± 0.029 (0.342)	$0.311^{+0.012}_{-0.014}$ (0.306)	0.297 ± 0.016 (0.309 0.311)	0.316 ± 0.011 (0.311)	0.311 ± 0.014 (0.317)
S_8	0.803 ± 0.018 (0.799)	$0.811^{+0.031}_{-0.039}$ (0.799)	0.746 ± 0.048 (0.842)	$0.639^{+0.043}_{-0.063}$ (0.711 0.864)	0.792 ± 0.015 (0.808)	0.790 ± 0.018 (0.814)
σ_8	$0.799^{+0.039}_{-0.047}$ (0.777)	$0.811^{+0.057}_{-0.076}$ (0.748)	0.733 ± 0.050 (0.833)	$0.643^{+0.043}_{-0.063}$ (0.701 0.849)	0.773 ± 0.024 (0.794)	$0.775^{+0.024}_{-0.028}$ (0.792)
w	-1	$-1.02^{+0.14}_{-0.19}$ (-0.81)	-1	$-1.17^{+0.13}_{-0.08}$ (≈ -1 -0.94)	-1	$-1.04^{+0.10}_{-0.08}$ (-0.93)
A_{ds}	0	-5^{+13}_{-20} (6)	0	-21^{+16}_{-10} (-22 0)	0	$-0.2^{+4.6}_{-5.9}$ (0.0)
h	-(0.677)	-(0.640)	0.681 ± 0.010 (0.676)	$0.713^{+0.018}_{-0.024}$ (0.678 0.664)	0.682 ± 0.009 (0.680)	$0.689^{+0.016}_{-0.020}$ (0.668)
n_s	-(0.904)	-(0.870)	$0.974^{+0.063}_{-0.055}$ (1.036)	0.945 ± 0.059 (1.022 1.049)	$0.957^{+0.041}_{-0.047}$ (0.977)	$0.955^{+0.041}_{-0.048}$ (0.985)
N_{par}	27	29	17(+32)	19(+32)	39(+32)	41(+32)
χ^2	511.9	509.8	470.03	469.7 468.9	513.4+469.4	513.2+468.8
χ^2_{prior}	9.5	9.3	7.99	7.5 8.3	19.6	18.9
log \mathcal{Z}	5749.2 ± 0.2	5748.8 ± 0.2	-123.3 ± 0.2	-126.9 ± 0.2	5630.5 ± 0.3	5627.8 ± 0.2

et al. 2023). This approach allows us to model the power spectrum multipoles in redshift space including mildly nonlinear scales. We use the same set-up of parameters and priors as in Carrilho et al. (2023). In the FS+BAO analysis the chosen priors on cosmological parameters are very broad and confined only by the Λ CDM cosmological parameter ranges of the linear *bacco* emulator (trained on CLASS outputs, Aricò et al. 2021). The only informative prior we impose is a Gaussian baryon (BBN) prior: $\omega_b \in \mathcal{N}(0.02268, 0.00038)$ (Aver et al. 2015; Cooke et al. 2018; Schöneberg et al. 2019). The priors on the DS parameters are specified by $w \in [-3, -0.5]$ and $A_{\text{ds}} \in [-500, 500]$ b GeV $^{-1}$. We compute the growth parameters in Λ CDM and DS scenarios using the *evogrowthpy* code.

We sample posterior distributions using Polychord (Handley et al. 2015) with the ‘publication quality’ parameters from Lemos et al. (2023). For the DS model we increase `live_points` and `num_repeats` to 1000 and 100 to guarantee sufficient sampling in the highly non-Gaussian posterior, with the ‘butterfly’-shaped prior in $w - A_{\text{ds}}$. To plot and derive constraints from the posterior distributions we use *getdist* (Lewis 2019). While for the best-fit, i.e. the Maximum *A Posteriori* (MAP) values, we use *iminuit* (James & Roos 1975). When the MAP value disagrees with the peak of the marginalised posterior obtained from the chain, it signifies the presence of projection effects (Gómez-Valent 2022; Hadzhiyska et al. 2023). Projection effects arise when a high-dimensional non-Gaussian posterior distribution is compressed in a lower-dimensional parameter space. Projection effects are especially prominent for extended cosmologies, in which beyond- Λ CDM parameters are strongly degenerate with cosmological parameters (Moretti et al. 2023; Maus et al. 2024). For a combination of probes with *CombineHarvesterFlow* we train and combine individual marginalised posterior-distributions in cosmological parameters $[\Omega_m, h, \omega_b, n_s, S_8, (A_{\text{ds}}, w)]$ with 14 flows (for details see Taylor et al. 2024). Additionally, we run a CMB analysis for DS using a modified version of CLASS and Cobaya with the Planck low- ℓ TT, the lollipop TE, EE and the lollipop TTTEEE likelihoods for the PR4 data release (Tristram et al. 2024). We do not include CMB lensing information to show constraints that are as independent as possible from the late-time data from LSS.

4 RESULTS

The constraints on cosmological parameters are given in Table 1 with the means, the 68 per cent credibility intervals, and the MAP values. We do not quote the constraints on ω_b as they are BBN-prior dominated for the FS and joint (3 \times 2pt+FS+BAO) analyses. In Figure 1 we show the posterior distributions of cosmological parameters in Λ CDM (left panel) and DS (right panel). For DS we omit n_s and h because it shows a trend similar to the Λ CDM case. Based on χ^2 statistics and comparison of the Bayes factors, the performance of both models is very similar, with no clear preference for Λ CDM or DS.

We first note that the DES-only re-analysis in Λ CDM yields a higher value of S_8 than the official results in Abbott et al. (2022b). This is due to our analysis choices listed in section 3 and in agreement with the DES shear re-analysis in Abbott et al. (2023a). DS expands the uncertainty on S_8 and drives the mean value higher, while the extended parameters are prior dominated and consistent with the Λ CDM-limit. However, the best-fit values in S_8 in both models are very close. The primordial amplitude computed at the MAP values equals to $\log 10^{10} A_s = 2.865$ in Λ CDM and $\log 10^{10} A_s = 3.042$ in DS. The latest CMB constraint without lensing information with Planck in PR4 for Λ CDM from Tristram et al. (2024) is $\log 10^{10} A_s = 3.040 \pm 0.014$. Our PR4 analysis with DS constraints the primordial amplitude to $\log 10^{10} A_s = 3.035 \pm 0.014$. From this we see that DS offers a solution that can consistently connect early-time measurements of the matter density fluctuations in the CMB with late-time LSS measurements. Additionally, our PR4 analysis with DS constraints the following parameters: $\omega_b = 0.0223 \pm 0.0001$, $\omega_c = 0.118 \pm 0.001$, and $n_s = 0.968 \pm 0.004$. However, it leaves the highly degenerated parameters w, A_{ds}, h unconstrained with CMB data alone.

The FS+BAO analysis reproduces the results of Carrilho et al. (2023) as expected with a strong shift in S_8 towards lower values in the marginalised posterior. Note that the authors quote best-fit values of the analytically marginalised posterior. Based on the MAP values (see Figure 2) we see that the shift is caused by the projection effects in both cosmologies; the data prefer higher values of S_8 than the

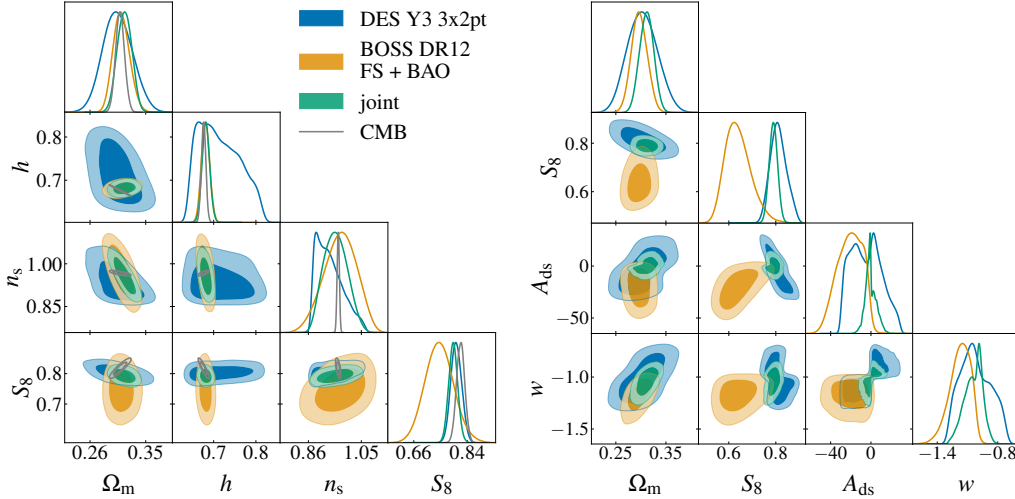


Figure 1. Marginalised posterior distribution for cosmological parameters in Λ CDM (left panel) and DS (right panel). Contours for DES Y3, BOSS DR12 and their combination are shown in blue, orange and green, respectively. Grey lines correspond to CMB constraints from [Tristram et al. \(2024\)](#) without lensing information.

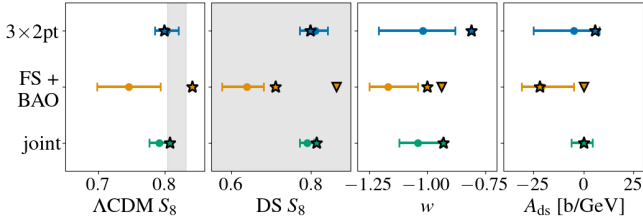


Figure 2. Projection effects in S_8 and the DS parameters. The error bars show the 68% marginalised posteriors, the stars denote the MAP values, the triangles denote the second-best MAP values in FS+BAO with DS. The grey shaded line corresponds to constraints on S_8 from CMB data ([Tristram et al. 2024](#)).

posterior averages. Moreover, from minimising the full posterior in DS we find very close χ^2 values that correspond to two very different values of the extended parameters. This implies that the data are not constraining enough to draw any conclusion about the DS constraints in this analysis setup.

In the joint (3 \times 2pt+FS+BAO) analysis for Λ CDM the S_8 -value remains slightly lower than the value extrapolated from the CMB measurements without lensing information. For instance, the tension is quantified by 1.9σ and 1.3σ with [Planck Collaboration et al. \(2020\)](#) and PR4, respectively. The corresponding primordial amplitude computed at the MAP values equals to $\log 10^{10} A_s = 2.975$. Meanwhile, DS constraints in the joint analysis are significantly improved, especially on A_{ds} . The corresponding primordial amplitude computed at the MAP values equals to $\log 10^{10} A_s = 3.029$. Similar to the DES-only analysis, in the joint analysis the MAP values are more in agreement with the CMB in DS than in Λ CDM.

In [Carrilho et al. \(2023\)](#) the authors demonstrated that CMB-informed priors on the primordial parameters, n_s and A_s , improve constraints on the extended parameters, decrease the shift in S_8 and the projection effects. As we show above, constraints on these parameters from the CMB in Λ CDM and DS are similar, hence the choice of the priors is justified. We find similar trends in the combination of the spectroscopic and photometric probes without CMB-informed priors

on the primordial parameters. In the joint analysis our constraints on A_{ds} have similar uncertainty, constraints on w are ~ 3 -times weaker, while S_8 constraints are ~ 2 -times stronger than the ones from the FS+BAO analysis with the informative priors. Additionally, in the joint analysis, the difference between the MAP and marginalised mean values is reduced (see [Figure 2](#)), signifying a decrease in the projection effects with respect to the individual LSS probes. This is also demonstrated in [Figure 3](#), where we vary the standard deviation of the Gaussian prior of the EFTofLSS nuisance parameters. The effects of enlarging the prior are small in Λ CDM: only lowering n_s and slightly decreasing S_8 . In DS, the shift towards lowest prior-bound in n_s is more prominent and resembles DES-only constraints for the largest EFTofLSS priors. We also observe a slight decrease in S_8 and increase in h . However, the ‘butterfly’-posterior in $w - A_{ds}$ around its Λ CDM-limit remains for all prior-choices. This implies that the photometric probes effectively constrain the amplitude of the power spectrum and help to break the degeneracy between S_8 and the extended parameters.

Finally, an application of the normalising flows approach in Λ CDM is straightforward and in agreement with the brute-force joint analysis (see [Figure 3](#)). For DS we have two complications: (a) the overlapping region in the marginalised S_8 -contours between the probes is small due to projection effects; (b) the ‘butterfly’-shaped posterior in $w - A_{ds}$ is highly non-Gaussian. To address these caveats we train the normalising flows on boosted posteriors (an approximation of true posteriors): this increases the size of the training set by approximately one order of magnitude. To better avoid projection effects in S_8 , we repeat the FS+BAO analysis with a flat prior on the primordial amplitude, $\log 10^{10} A_s \in [2.6, 4]$, motivated by the results of the DES-only analysis. We also re-run the DES analysis by imposing a BBN prior (this is known to improve `CombineHarvesterFlow` performance, see [DESI Collaboration et al. 2024](#)). Overall, we reach a good agreement between the brute-force combination and the normalising flows approach with the boosted posterior distributions and adjusted A_s -prior runs. `CombineHarvesterFlow` successfully passes this stress-test on highly non-Gaussian posterior distributions with strong projections.

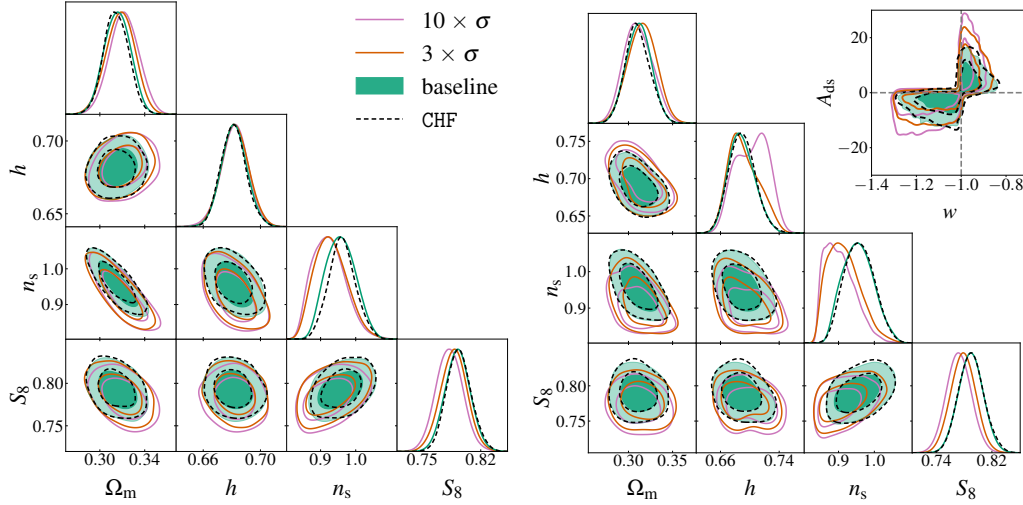


Figure 3. Marginalised posterior distribution for cosmological parameters in the joint Λ CDM (left panel) and DS (right panel) analyses for three different choices for the priors on EFTofLSS nuisance parameters: baseline case (green) and the cases with standard deviations of nuisance parameters, except for b_1 , increased by factors of 3 (orange) and 10 (pink). Dashed black line shows baseline joint analysis with the normalising flow, `CombineHarvesterFlow` (CHF), approach.

5 CONCLUSIONS

In this letter we combine photometric and spectroscopic probes from Stage III surveys: the 3x2pt correlation functions of DES Y3, and the FS+BAO measurements of BOSS DR12, including external BAOs. The methods and findings of this study are important for forthcoming beyond- Λ CDM analyses by Stage-IV surveys like DESI, Euclid, and Rubin, which will simultaneously provide spectroscopic and photometric datasets with unprecedented precision. Currently, the significance of the apparent S_8 tension between the CMB and joint LSS analysis for Λ CDM depends on the reference CMB data (see, e.g. [Tristram et al. 2024](#); [Roy Choudhury & Okumura 2024](#)). For instance, for our analysis setup the tension is reduced to $\sim 1.3\sigma$ when compared with Planck PR4 within the standard cosmology. In case the tension would remain with Stage-IV data, Dark Scattering (DS), an interacting dark energy model, presents a potential resolution. Here we provide the first DS constraints from DES Y3 data, from the joint analysis of DES Y3 and BOSS DR12, and from Planck PR4 data. The joint analysis constraints on the DS parameters are $w = -1.04^{+0.10}_{-0.08}$ and $A_{\text{ds}} = -0.2^{+4.6}_{-5.9} \text{ b GeV}^{-1}$. There is no significant detection of DS. However, in the DES-only and joint analyses, the MAP-values of the model demonstrate an exemplary solution of the tension. We also show that the joint LSS analysis without CMB information is comparable with the single-probe BOSS analysis with CMB-informed priors. The combination of probes allows minimising the projection effects without the inclusion of CMB information: it brings the marginalised posterior maxima closer to the corresponding best-fit values and weakens the sensitivity to the priors of the EFTofLSS nuisance parameters. Finally, we find good agreement between the direct joint analysis and the combination of posteriors via normalising flows.

ACKNOWLEDGEMENTS

The authors are grateful to the BOSS and DES collaborations for making their data publicly available. MT’s research is supported by grant ST/Y000986/1. SL and KM are grateful for funding from JPL’s R&TD 7x ‘Future of Dark Sector Cosmology: Systematic Ef-

fects and Joint Analysis’ (01STRS/R.23.312.005). AP is a UK Research and Innovation Future Leaders Fellow (grant MR/X005399/1). PC’s research is supported by grant RF/ERE/221061. CM’s work is supported by the Fondazione ICSC, Spoke 3 Astrophysics and Cosmos Observations (Project ID CN_00000013). BB is supported by a UK Research and Innovation Stephen Hawking Fellowship (EP/W005654/2). PLT is supported in part by ‘NASA ROSES 21-ATP21-0050’. A part of this research was carried out at the Jet Propulsion Laboratory, California Institute of Technology, under a contract with the National Aeronautics and Space Administration (80NM0018D0004). For the purpose of open access, the author has applied a Creative Commons Attribution (CC BY) license to any Author Accepted Manuscript version arising from this submission.

DATA AVAILABILITY

Links and references with sources of the data and analysis pipelines are provided in the main text.

REFERENCES

- Abbott T. M. C., et al., 2022a, *Phys. Rev. D*, **105**, 023520
- Abbott T. M. C., et al., 2022b, *Phys. Rev. D*, **105**, 023520
- Abbott T. M. C., et al., 2023a, *Open J. Astrophys.*, **6**, 2305.17173
- Abbott T. M. C., et al., 2023b, *Phys. Rev. D*, **107**, 083504
- Alam S., et al., 2015, *The Astrophysical Journal Supplement Series*, **219**, 12
- Aricò G., et al., 2021, *arXiv e-prints*, p. arXiv:2104.14568
- Aricò G., et al., 2023, *Astron. Astrophys.*, **678**, A109
- Asgari M., et al., 2021, *Astron. Astrophys.*, **645**, A104
- Aver E., et al., 2015, *J. Cosmology Astropart. Phys.*, **2015**, 011
- Baldi M., Simpson F., 2015, *MNRAS*, **449**, 2239
- Baldi M., Simpson F., 2017, *MNRAS*, **465**, 653
- Baumann D., et al., 2012, *J. Cosmology Astropart. Phys.*, **2012**, 051
- Beutler F., et al., 2011, *MNRAS*, **416**, 3017
- Beutler F., et al., 2017, *MNRAS*, **466**, 2242
- Blas D., et al., 2011, *J. Cosmology Astropart. Phys.*, **2011**, 034
- Bose B., Taruya A., 2018, *JCAP*, **10**, 019
- Bose B., et al., 2018, *J. Cosmology Astropart. Phys.*, **2018**, 032
- Bose B., et al., 2020, *Mon. Not. Roy. Astron. Soc.*, **498**, 4650

- Carrasco J. J. M., et al., 2012, *Journal of High Energy Physics*, 2012, 82
- Carrilho P., et al., 2021, *J. Cosmology Astropart. Phys.*, 2021, 004
- Carrilho P., et al., 2022, *Mon. Not. Roy. Astron. Soc.*, 512, 3691
- Carrilho P., et al., 2023, *J. Cosmology Astropart. Phys.*, 2023, 028
- Carrion K., et al., 2024, *MNRAS*, 532, 3914
- Cataneo M., et al., 2019, *Mon. Not. Roy. Astron. Soc.*, 488, 2121
- Cooke R. J., et al., 2018, *ApJ*, 855, 102
- D'Amico G., et al., 2020, *JCAP*, 05, 005
- DESI Collaboration et al., 2024, *arXiv e-prints*, p. arXiv:2411.12022
- Fonseca de la Bella L., et al., 2017, *J. Cosmology Astropart. Phys.*, 2017, 039
- Friedrich O., et al., 2021, *Mon. Not. Roy. Astron. Soc.*, 508, 3125
- Gil-Marín H., et al., 2016, *MNRAS*, 460, 4188
- Gómez-Valent A., 2022, *Phys. Rev. D*, 106, 063506
- Hadzhiyska B., et al., 2023, *The Open Journal of Astrophysics*, 6, 23
- Handley W. J., et al., 2015, *Mon. Not. Roy. Astron. Soc.*, 450, L61
- Heymans C., et al., 2021, *A&A*, 646, A140
- James F., Roos M., 1975, *Comput. Phys. Commun.*, 10, 343
- Joachimi B., et al., 2021, *Astron. Astrophys.*, 646, A129
- Kitaura F.-S., et al., 2016, *MNRAS*, 456, 4156
- Krause E., et al., 2021, *arXiv e-prints*, p. arXiv:2105.13548
- Lemos P., et al., 2023, *Mon. Not. Roy. Astron. Soc.*, 521, 1184
- Lesgourgues J., 2011, *arXiv e-prints*, p. arXiv:1104.2932
- Lewis A., 2019, *arXiv e-prints*, p. arXiv:1910.13970
- Lewis A., Challinor A., 2011, *CAMB*, ascl:1102.026
- Linton M. S., et al., 2022, *JCAP*, 08, 075
- Maus M., et al., 2024, *arXiv e-prints*, p. arXiv:2404.07312
- Mead A., et al., 2021, *Mon. Not. Roy. Astron. Soc.*, 502, 1401
- Moretti C., et al., 2023, *J. Cosmology Astropart. Phys.*, 2023, 025
- Oddo A., et al., 2020, *J. Cosmology Astropart. Phys.*, 2020, 056
- Oddo A., et al., 2021, *J. Cosmology Astropart. Phys.*, 2021, 038
- Palma D., Candlish G. N., 2023, *Mon. Not. Roy. Astron. Soc.*, 526, 1904
- Perko A., et al., 2016, *arXiv e-prints*, p. arXiv:1610.09321
- Philcox O. H. E., 2021a, *Phys. Rev. D*, 103, 103504
- Philcox O. H. E., 2021b, *Phys. Rev. D*, 104, 123529
- Philcox O. H. E., Ivanov M. M., 2022, *Phys. Rev. D*, 105, 043517
- Planck Collaboration et al., 2020, *A&A*, 641, A6
- Porredon A., et al., 2021, *Phys. Rev. D*, 103, 043503
- Porredon A., et al., 2022, *Phys. Rev. D*, 106, 103530
- Pourtsidou A., Tram T., 2016, *Phys. Rev. D*, 94, 043518
- Pourtsidou A., et al., 2013, *Phys. Rev. D*, 88, 083505
- Rizzo F., et al., 2023, *J. Cosmology Astropart. Phys.*, 2023, 031
- Rodríguez-Torres S. A., et al., 2016, *MNRAS*, 460, 1173
- Ross A. J., et al., 2015, *MNRAS*, 449, 835
- Roy Choudhury S., Okumura T., 2024, *ApJ*, 976, L11
- Sánchez C., et al., 2022, *Phys. Rev. D*, 105, 083529
- Schöneberg N., et al., 2019, *J. Cosmology Astropart. Phys.*, 2019, 029
- Simpson F., 2010, *Phys. Rev. D*, 82, 083505
- Skordis C., et al., 2015, *Phys. Rev. D*, 91, 083537
- Spurio Mancini A., Pourtsidou A., 2022, *MNRAS*, 512, L44
- Spurio Mancini A., et al., 2022, *Mon. Not. Roy. Astron. Soc.*, 511, 1771
- Taylor P. L., et al., 2024, *The Open Journal of Astrophysics*, 7, 86
- Tristram M., et al., 2024, *A&A*, 682, A37
- Tsedrik M., et al., 2023, *MNRAS*, 520, 2611
- du Mas des Bourboux H., et al., 2020, *ApJ*, 901, 153

This paper has been typeset from a $\text{\TeX}/\text{\LaTeX}$ file prepared by the author.